The Concept of "Attractive Region in Environment" and its Application in High-Precision Tasks With Low-Precision Systems

Hong Qiao, *Senior Member, IEEE*, Min Wang, Jianhua Su, Shengxin Jia, and Rui Li

***Abstract*—High-precision manipulation is very important for a variety of tasks in manufacturing. In general, high-precision manipulation is usually achieved by the guidance of high-precision sensors; however, sensorless methods, for some special cases, are more reliable and effective. There are many important works in this aspect [1]–[3]. The concept of "attractive region in environment" (ARIE), which was proposed in our previous works [4]–[6], provides a prospective approach for low-precision systems to achieve high-precision manipulation. It has been used in various industrial applications, such as robotic assembly [7], grasping [8], and localization [9]. ARIE is a region from any point of which the uncertainty of the system can be eliminated by a state-independent input. The utilization of attractive region can be easily understood by the case of a bean in a bowl. For a bean in a bowl, no matter where the initial position of the bean is, it will move to and finally stay at the bottom of the bowl under gravity. Thus, the uncertainty of the bean is eliminated by gravity without any sensor feedback. Inspired by the above case, the general concept of ARIE is proposed and is applied to industry. In this paper, we review the application of ARIE and give its formal definition. Furthermore, we establish conditions for the existence of ARIE in the generalized configuration space, which is complex and nonideal. The relationship between the high-dimensional attractive region and the low-dimensional one is also discussed, which is helpful to make feasible and reliable manipulation strategies in the low-dimensional configuration space. The main contribution of this paper is the generalization of the concept of ARIE, which provides a theoretical foundation for applications including the high-precision manipulation with low-precision system. The experimental simulations on different kinds of complex manipulations show the effectiveness of the proposed method for industrial applications.**

***Index Terms*—Assembly, attractive region in environment (ARIE), grasping, localization, sensorless manipulation.**

Manuscript received December 31, 2013; revised September 14, 2014; accepted October 11, 2014. Date of publication December 18, 2014; date of current version August 24, 2015. Recommended by Technical Editor Z. Xiong. The work of H. Qiao was supported in part by the National Natural Science Foundation (NNSF) of China under Grant 61033011 and Grant 61210009. The work of M. Wang was supported in part by the NNSF of China under Grant 61303174. The work of J. Su was supported in part by the NNSF of China under Grant 61105085.

H. Qiao, M. Wang, and J. Su are with the State Key Lab of Management and Control for Complex Systems, Institute of Automation, Chinese Academy of Sciences, Beijing 100190, China (e-mail: hong.qiao@ia.ac.cn; min.wang@ia.ac.cn; jianhua.su@ia.ac.cn).

S. Jia is with the University of California, Los Angeles, CA 90095 USA (e-mail: shengxin.jia@bath.edu).

R. Li is with the Graduate School and the State Key Laboratory of Management and Control for Complex Systems, Institute of Automation, Chinese Academy of Sciences, Beijing 100190, China (e-mail: rui.li@ia.ac.cn).

Color versions of one or more of the figures in this paper are available online at http://ieeexplore.ieee.org.

Digital Object Identifier 10.1109/TMECH.2014.2375638

I. Introduction

How to achieve high-precision manipulation with a low-precision system is a key problem in manufacturing. In general, it is believed that this can only be achieved with rich sensor information. So far, sensor feedback has been widely used to eliminate the uncertainty of a system. However, there are also many problems caused by sensor systems; for example, 1) a sensor system increases the initial cost to the system; 2) a sensor system reduces the robustness and reliability of the whole system; 3) in certain cases, the states measured by sensors may be different from that needed [10]; and 4) in other situations, sensors may not be able to provide enough precision. Moreover, due to the high cost and maintenance difficulty of high-precision sensors, many tedious works still need to be done manually or with low-precision sensors. Therefore, research on low-precision systems that use few sensors or even no sensors to achieve high-precision tasks is very important for manufacturing.

Sensor-based manipulation exists in many application areas. Force information is usually used to achieve peg-hole insertion when the inaccuracy of manipulator positioning exceeds assembly tolerances [11]. Force sensors have been successfully utilized in round peg-hole insertion [12], [13], noncylinder peg-hole insertion [14], and multipeg-hole insertion [15]. Sensor information can also be applied to object localization. Faugeras and Hebert used the ranged data to recognize and locate a 3-D object from a set of shape-known objects [16]. Najdovski *et al.* designed a novel pinch grasp based on force sensor for the manipulation of micro/nano objects [17]. Xin *et al.* introduced a new swirl gripper with force sensors to evaluate the pressure distribution when grasping [18]. Backus and Dollar proposed a compliant structure with contact sensors for target contact detection based on resonant frequency [19]. Recently, 3-D sensing techniques, such as laser sensors, photoelectric sensors, and multiview stereo vision, have shown their potential ability in providing more robust solutions for object localization in industrial environment [20]–[24].

On the other hand, manipulations without or with few sensors have been investigated for many years. Some works focus on eliminating the uncertainty of the system based on limited sensor information. Canny and Goldberg discussed the manipulations with reduced intricacy in sensing and control [25], such as light beam sensors and parallel-jaw grippers. They showed that such a system was capable of recognizing and orienting a broad class of industrial parts. Erdmann generated the strategies for robot tasks by using a back-chaining planner [26], in which

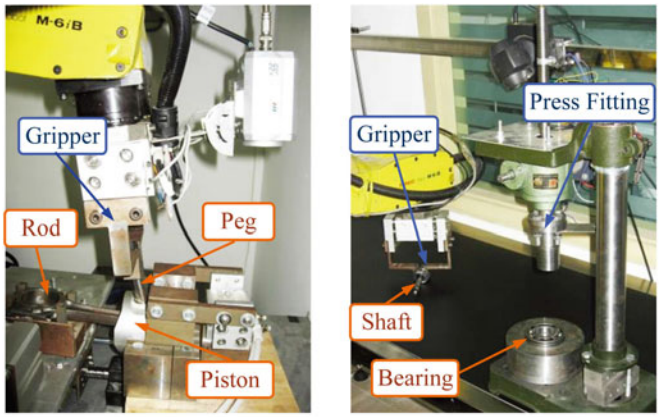

Fig. 1. Round-peg-hole insertion is a typical operation in automatic manufacturing. (a) Peg-rod-piston insertion for the engine assembly, and (b) Shaft-bearing insertion. In (b), the gripper is grasping the shaft upper end, and the press fitting is used for the pressing at the last procedure of assembly.

the sensors need to provide only the information required for the plan to function correctly instead of actually perfect information. Taylor described a task-level manipulator planning system that could generate a skeleton plan [27]. Based on the skeleton plan, the position uncertainties could be eliminated or be bounded by a serial of sensing operations. Some researchers also made use of constraints of the environment instead of additional devices to achieve high-precision operation, such as Caine *et al.* [28] and Matsuno *et al.* [29], and the use of compliant motions to eliminate the uncertainty has been reviewed in [30]. Recently, sensorless robotic manipulation for object localization or grasping is also a popular topic in robotic application. Zhang *et al.* proposed an algorithm to reorient some polyhedral parts from some initial orientations to a unique orientation [31]. Marigo *et al.* adopted a dexterous mechanism to rotate a polyhedron around its edges from a given configuration to another reachable configuration with minimal complexity [32]. Erdmann and Mason explored the use of sensorless manipulation strategies to eliminate the uncertainties in the orientation of a part by repeated tilts of tray [33]. They developed a planner that used the knowledge of mechanics of sliding to predict the results of actions. Goldberg and his collaborators developed several methods on the sensorless object orienting or feeding [34]–[36], where the optimal and suboptimal strategies were given to recognize a part from a known set of parts by grasping it and sensing its diameter function. Some other researchers aimed to study the placements of fingers that prevent a polygon moving arbitrarily from a given position, where no sensors are needed. A typical example is the caging problem originally given by Kuperberg [37]. Davidson *et al.* [38], Pipattanasomporn and Sudsang[39], and Rodriguez *et al.* [40] extended this technique to the calculation of the caging set for different 2-D objects. Another important concept of finding the initial region for grasping is independent contact region (ICR) [41], which originally addresses the problem of finding the largest ICR on the surface of a polyhedron to ensure a force-closure grasp. Roa *et al.* extended this approach to compute ICRs with any number of frictionless or frictional contacts on the surface of a 3-D object [42].

In our previous work, we used the constrained region formed by environment, which is called the "attractive region in environment" (ARIE), to eliminate the uncertainty of the system and to achieve high-precision and high-reliability tasks, including assembly, grasping, and localization. 1) For the assembly application, we identified the basic relationship among the inputs to the peg-hole system, the movements of the peg and the contact forces between the peg and the hole [43]. Then a theoretical model for the peg-hole aligning search was proposed to reduce the angular and translational errors during the insertion processing. The range of the peg movement was also analyzed, which was useful in the subgoals programming for the insertion operation. Thus, high speed, high accuracy round-peg-hole insertion [44], and triangular object insertion [45] were successfully realized. Moreover, we also applied the strategy to the manufacturing processes, such as the piston-rod-peg insertion of a car engine [7], and the eccentric peg-crankshaft insertion of a car compressor [46]. 2) In the application to grasping, the ARIE can be used to guide a stable grasp, where the rigorous placements of the gripper are not necessary. Based on the concept of ARIE, a strategy was formulated to rotate a polygonal part from any initial position to a certain orientation in an obstacle-free plane [9]. 3) For localization, the ARIE can be used to analyze the configuration space of an object on a flat plane. With a new coordinate system, the proposed robotic manipulating system can localize the object from any initial state to a fixed state based on the ARIE [6], [9].

In this paper, we will give a theoretical analysis of the attractive region constrained by the environment. Specifically, we will first analyze three examples in robotic manipulations, from each of which the attractive region can be derived, and then establish conditions for the existence of the attractive regions in different configuration spaces. The main contribution of this paper can be concluded as follows.

1) We give a theoretical generalization of the concept of ARIE, which provides a theoretical foundation for the application of high-precision manipulation with low-precision systems. Compared with our previous work [4]–[9], where simple and desired configuration spaces are obtained, the concept of ARIE can be extended to the situations where a more complex and nonideal configuration space exists.
2) We analyze the existence and identification method of the ARIE in different kinds of configuration spaces. Due to the wide existence of the high-dimensional ARIE in industrial manipulation, an application strategy is introduced based on the relationship between the high-dimensional ARIE and the low-dimensional one, which can be easily applied for practical tasks.
3) Implementation of the manipulation tasks is carried out to verify the effectiveness of the proposed theoretical foundation of the ARIE. Simulations on nonideal or high-dimensional ARIE show the robustness of the proposed method for the wide and high-precision manipulation without sensor information.

The rest part of this paper is arranged as follows. Section II describes three examples of industrial applications in which the concept of ARIE can be applied, including robotic assembly,

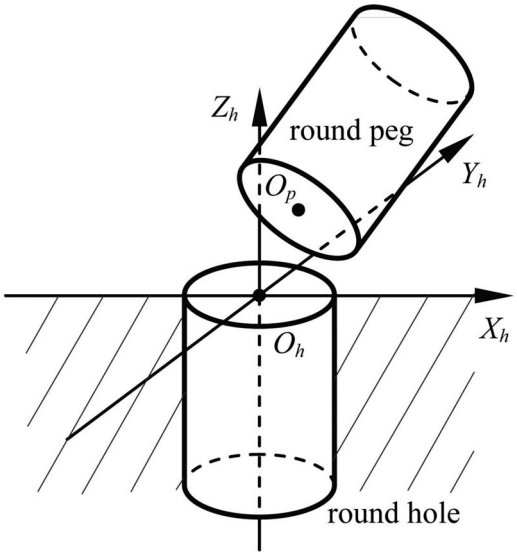

Fig. 2. Coordinate frame established for the round-peg-hole insertion. Base point O_h is defined as the center of the hole's upper surface.

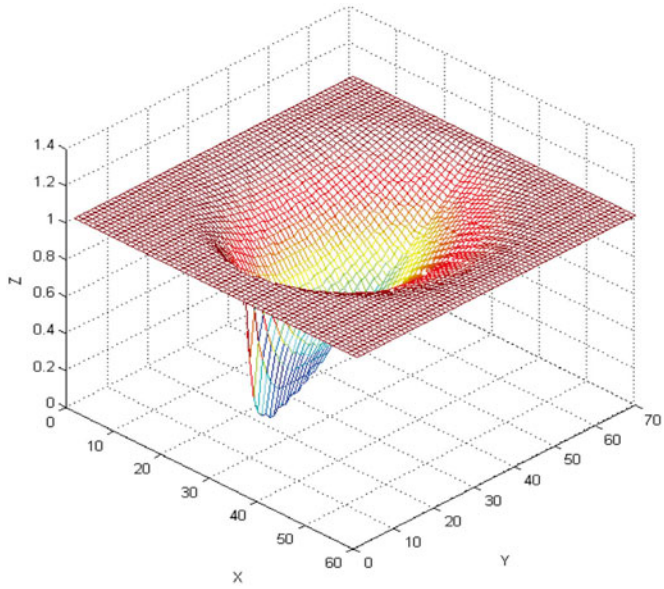

Fig. 3. Configuration space of the round peg formed by the constraints of a round hole.

grasping, and localization. Section III introduces the generalization of ARIE, which is presented based on the theoretical analysis. In Section IV, a general method of visualizing the high-dimensional attractive region through mapping a high-dimensional space into its subspaces is proposed. Section V mentions some typical applications of the ARIE in assembly for industrial manufacturing. Section VI gives some conclusions and discusses some future work on attractive regions, such as its application in face recognition.

II. General Concept of "ARIE"

In this section, three specific applications in robotic manipulation are analyzed to introduce the ARIE. Based on the attractive region, it is capable to achieve high-precision tasks (e.g., the peg-hole insertion, 3-D object grasping, and 3-D polyhedral object localization) with a low-precision robotic system.

A. Example 1: Round-Peg and Round-Hole Insertion

The peg-hole assembly operation is very difficult but necessary for automatic manufacturing. A typical operation is the round-peg-hole insertion (see Fig. 1), whose objective is to insert a round peg into a round hole with high precision [13], [15], [47], [48].

As shown in Fig. 2, a coordinate frame is fixed on the hole to describe the peg-hole relation. The base point O_h of the coordinate is defined as the center of the upper surface of the hole, the axis O_hX_h is fixed on the line from O_h to the base of the robot, the axis O_hZ_h is along the axis of the hole upwards, and the axis O_hY_h is perpendicular to O_hX_h and O_hZ_h and satisfies the right-hand rule with them.

Then, the position of the peg in the coordinate frame built up based on the hole can be described as follows:

$$P_{\text{peg}} = \left[|O_hO_p|_{X_h}, |O_hO_p|_{Y_h}, |O_hO_p|_{Z_h}, \theta_{X_h}, \theta_{Y_h}, \theta_{Z_h} \right]^T \in C^6 \tag{1}$$

where C^6 is the constrained region formed by the edge of the hole in $\mathbb{R}^6$. For simplicity, we let $x = |O_hO_p|_{X_h}$, $y = |O_hO_p|_{Y_h}$, $z = |O_hO_p|_{Z_h}$. If the angle $[\theta_{X_h}, \theta_{Y_h}, \theta_{Z_h}]$ between the peg and the hole are fixed, then the movement of the peg can be described in $\mathbb{R}^3$, that is

$$P_{\text{peg}} = [x, y, z]^T \in C^3. \tag{2}$$

As shown in Fig. 3, the motion region of the peg constrained by the edge of the hole has a lowest-lying point, which is globally unique. This point is corresponding to the state of three-point contact denoted as the stable state of the assembly system, and is significant for the insertion.

This constrained region reminds us of a visualized example in the physical space. If there is a bowl with a bean inside, and the goal is to put the bean to the bottom of the bowl, then no matter where the initial position of the bean is, with help of the gravity, the bean will move to and is finally stabilized at the bottom of the bowl.

For round-peg-hole insertion, the peg is similar to the "bean," and the motion region of the peg formed by constraints of the hole edge is similar to the "bowl." Then, it is possible to design a state-independent input $u(t)$ for the peg to reduce the uncertainty of the system, just like the gravity for the bean in the bowl.

B. Example 2: Grasping With a Four-Pin Gripper

Generally, a stable grasp of an object is the most desirable behavior in robotic manipulation. Though the dexterous multifinger gripper with multiple degrees of freedom is still in an experimental stage, using a four-pin gripper with one-parameter is the easiest way to achieve form closure and to confine the object to a locally unique pose [see Fig. 4(a)].

We now focus on the analysis of grasping a 2-D rectangular object with a four-pin gripper [4], [8]. We establish a coordinate frame for the rectangular object and the four pins of the gripper

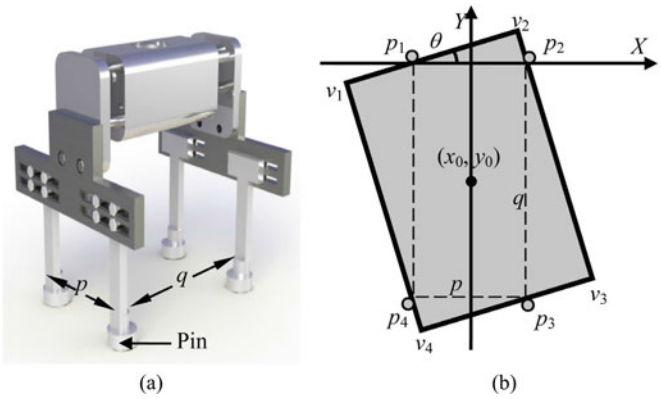

Fig. 4. Grasping with a four-pin gripper. (a) Four-pin gripper with fixed distance p between two pins at the same side and changeable distance q between the two sides. (b) Coordinate frame established for grasping a rectangular object with this gripper.

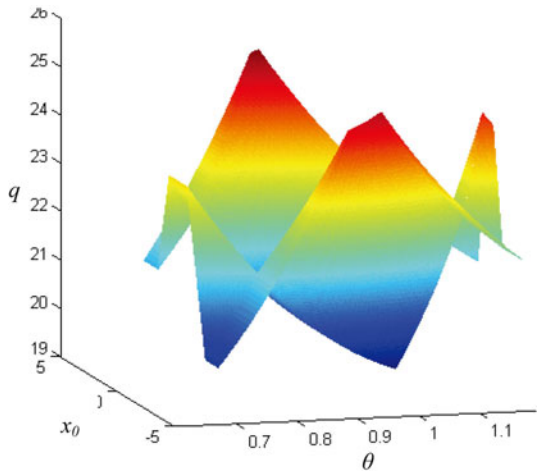

Fig. 5. Configuration space formed by the grasping action to a rectangular object [8]. Due to that y_0 is a function of x_0 and θ, this constrained region can be described by x_0, θ, and q for easier visualization.

in Fig. 4(b), where $\overrightarrow{p_1p_2}$ and $\overrightarrow{p_4p_3}$ are two pairs of parallel pins with the same interval. The *X*-axis is along the direction of $\overrightarrow{p_1p_2}$, and the *Y*-axis is perpendicular to the *X*-axis at the middle point of $\overrightarrow{p_1p_2}$. The vertex of the rectangle object is denoted by v_i, $i = 1, 2, 3$, and 4. The angle between $\overrightarrow{p_1p_2}$ and $\overrightarrow{v_1v_2}$ is θ, and the coordinate of the object's center is defined as (x_0, y_0). The distance between the two sides of the gripper is q.

For a form closure state, x_0, y_0, and θ are uniquely determined and q reaches its local minimum. Therefore, a constrained region exists in the configuration space of the system described by $[x_0, y_0, \theta, q]^T$. Then, the constrained region of q is a function of $[x_0, y_0, \theta]^T$, that is

$$q = f(x_0, y_0, \theta). \tag{3}$$

The constrained region of q is illustrated in Fig. 5. The surface of the region represents the closure state of grasping. It can be seen that q actually has a lowest value in the region. If the frictional coefficient of the contact points is small enough, the grasping state will move from an initial point in the constrained region to the point with the minimum q, where the uncertainties of $[x_0, y_0, \theta]^T$ are eliminated. This action can be achieved just by closing the gripper.

Hence, for grasping with the four-pin gripper, the object is similar to the "bean," and the motion region of the object relying on the constraints of gripper forms the "bowl." Moreover, the closing force of the gripper acting on the object plays a role as the gravity did to the "bean."

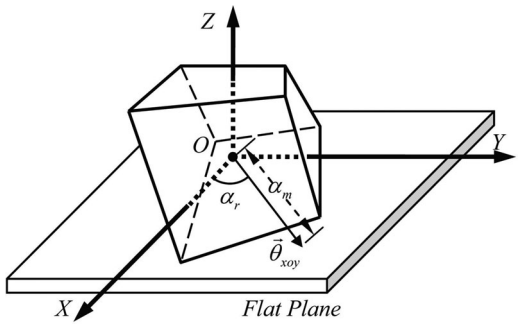

Fig. 6. *OXYZ*-coordinate system for object localization [9]. The state of the object on the flat plane can be represented by the rotation angle of the object around *Z*-axis and the angular vector $\vec{\theta}_{xoy}$ between the object with *XOY*-plane of the coordinate. α_r and α_m are the direction and length of $\vec{\theta}_{xoy}$, respectively.

C. Example 3: Sensorless Localization of 3-D Parts

Localization is an important step in manufacturing, which can be considered as a prior process of assembly, machining, transportation, etc. Compared with localization using sensors, localization without sensors can be cheaper and more reliable, and has lower requirements on the environment.

Now we give an example of localizing an object on a flat plane to illustrate the potential constrained region in this procedure. As shown in Fig. 6, a new kind of coordinate frame *OXYZ* is specially defined for object localization as follows.

The origin O of the coordinate frame is fixed on the center of gravity (c_g) of the 3-D object, and will move together with c_g when the object is moving. The *Z*-axis is perpendicular to the supporting plane of the object and points upward. Hence, the *XOY*-plane is parallel to the supporting plane, but the directions of the *X*-axis and *Y*-axis are not fixed. The two axes will rotate along with the object when the object is rotating around the *Z*-axis, and they will not change if the object rotates around any line through the origin *O* on the *XOY*-plane, such as $\vec{\theta}_{xoy}$.

In this coordinate frame, the object stabilized at the supporting plane with any initial state can reach every contact state of the object touching the supporting plane by two kinds of rotations: rotating around the *Z*-axis, and rotating around a certain vector on the *XOY*-plane. Detailed explanations could be found in [6] and [9].

Specifically, we let α_r denote the angle between $\vec{\theta}_{xoy}$ and *X*-axis, let α_m denote the length of $\vec{\theta}_{xoy}$, and let d represent the radius function, which is the distance between c_g and the flat plane. Then the contact state of the object touching the flat plane can be uniquely represented by

$$P_{obj} = [\alpha_r, \alpha_m, d]^T. \tag{4}$$

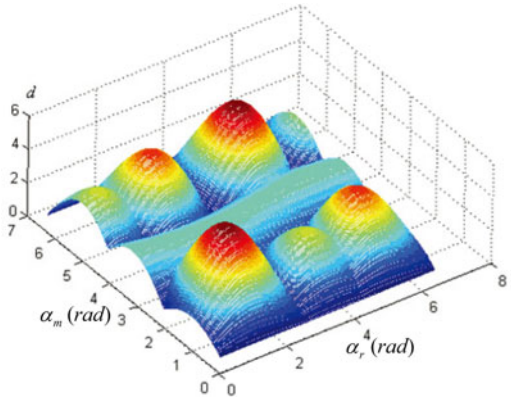

Fig. 7. Formative configuration space of $[\alpha_r, \alpha_m, d]^T$ which denotes the contact state of a tetrahedron touching the flat plane [9].

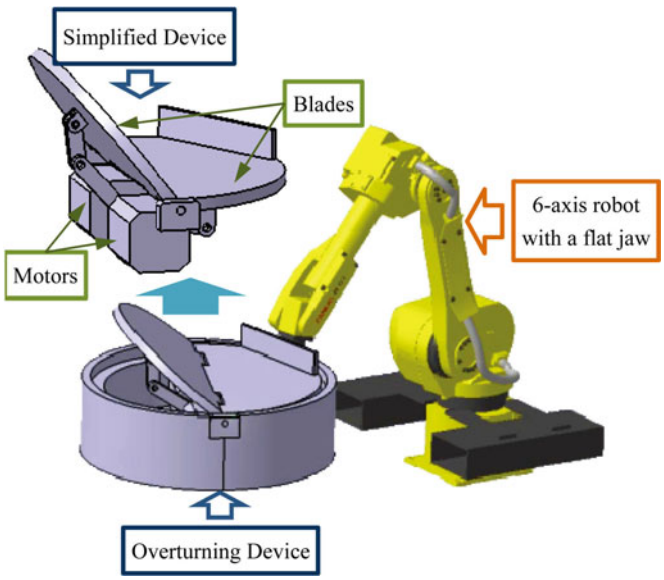

Fig. 8. Localization system with a manufacturing robot and an overturning device [9]. The overturning device, which can be simplified as the device illustrated on the upper left, is used to change the contact phases between the object and blades.

As shown in Fig. 7, different from the two examples above, it can be seen that there are multiple local extremes in the configuration space. In order to achieve high-precision localization, we need to design a series of state-independent input $u_a(t)$. So that the state of the system will converge as time passes, that is, the uncertainty of the system is eliminated.

In our previous work [9], we designed a robotic manipulating system for the localization of work pieces, as shown in Fig. 8. The localization operation is implemented based on the coordinate frame and the configuration space proposed above. Based on this system, an object can be localized to a unique state from an arbitrary initial state by some overturning and shifting operations without any sensor.

In summary, similar constrained regions are obtained in the configuration space of the manipulation system for assembly, grasping, and localization, as shown in Figs. 3, 5, and 7. Extensive studies have been done in our previous work [4], [8], [9] on the formulation of the desired attractive region (the bowl-like region) based on the constraints of environment for different kinds of application. Further theoretical analysis and generalization of the concept of ARIE are given in the next section, which is significantly helpful for the wide application to the systems with a general configuration space.

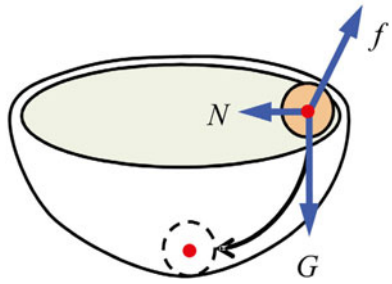

Fig. 9. Motion of a bean under the constraints of a bowl. The bean will finally converge to the bottom of the bowl under the effect of three forces, gravity G, frictional force f, and support force N.

III. General Formulation of "ARIE"

In this section, we will further analyze the properties of the constrained region mentioned above and give the definition of the concept of attractive regions. Then, several cases of attractive regions are given and a method for identification is also summarized. Finally, we generally analyze the correspondence between a point on the attractive region and the physical manipulation state.

A. Formulation of the Attractive Region From the Three Examples

As discussed in Section II, a bowl-like constrained region widely exists in the configuration space of manufacturing systems, such as the peg-hole insertion, four-pin grasping, and object localization. Therefore, if we can make a full use of the bowl-like region, many kinds of high-precision tasks will be achieved.

Based on the consideration above, we focus on the analysis of the "bean-bowl" system. As illustrated in Fig. 9, this kind of constrained regions is similar to the situation with a bean inside a bowl. The bean on the bowl is affected by three forces, the gravity G, the frictional force $f(x_1, x_2, N)$, and the support force $N(x_1, x_2, G)$, where x_1 and x_2 are the parameters corresponding to the position-like and velocity-like states. Under the effect of gravity, which is a state-independent input to the "bean-bowl" system, the state of the bean will finally converge to the goal region (the bottom of the bowl). It should be noted that the size of the goal region is smaller than that of the possible initial region, that is, the uncertainty of the system is reduced.

With the analysis above, we first give the definition of ARIE based on the bowl-like constrained region. The condition of the existence of ARIE in a nonlinear system is presented as follows [4], [6].

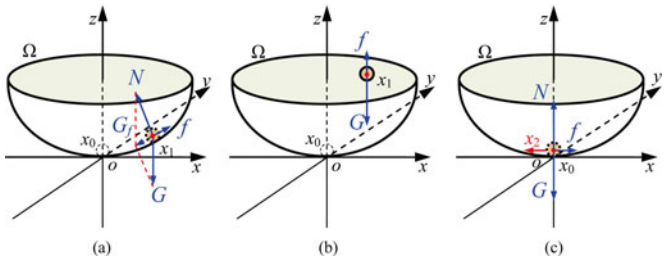

Fig. 10. Three different situations of the state point in a bowl-like region. In (a), (b), and (c), the state point is on the surface, in the inner space and at the lowest point of the region, respectively.

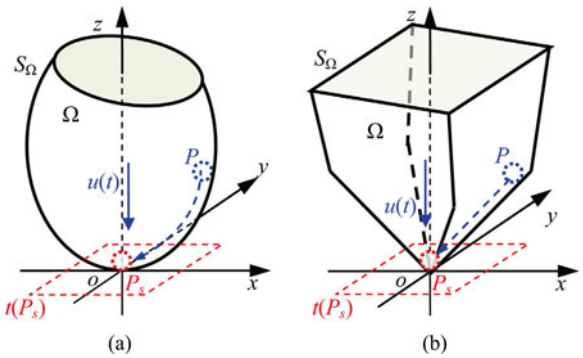

Fig. 11. Coordinate frame built up for the convex domain. The convex domain in (a) is smooth and the one in (b) has several vertices.

Definition 1: Assume that the state of a system can be characterized as $\mathrm{d}x/\mathrm{d}t = f(x,u)$ with $x(t) \in X$, where $x(t)$ is the state of the system and X is a region. For a region $\Omega \subset X$, if for all x in Ω, there exists a state-independent input $u(t)$ and a certain function $g(x)$ satisfying that

1) $g(x) > g(x_0)$, when $x \neq x_0$, and $g(x) = g(x_0)$, when $x = x_0$;
2) $g(x)$ has continuous partial derivatives with respect to all components of x,

then the system will be stable in the region Ω, and Ω is called the ARIE.

Remark 1: In Definition 1, Ω is a constrained region in the configuration space formed by the system $\mathrm{d}x/\mathrm{d}t = f(x,u)$ with $x(t) \in X$.

Remark 2: Assume that a constrained region Ω in the configuration space is bounded by a function $S(x)$. If $S(x)$ has no local minima then, by Definition 1, the region Ω is not ARIE since there is no lowest point x_0 so that no input $u(t)$ can be found to push any point x in Ω to converge to the point x_0 with the constraint of $S(x)$. Conversely, even if $S(x)$ has local minima, the region Ω is not necessarily an ARIE (see Theorem 3 below).

In the following, general cases of the attractive regions will be discussed through several theorems.

B. Several General Cases of "ARIE"

As mentioned above, the bowl-like region in $\mathbb{R}^3$ is a typical ARIE, which also widely exists in the configuration space of manufacturing systems. Therefore, we first focus on the analysis of this kind of constrained regions.

Theorem 1: A bowl-like region in the configuration space is a kind of ARIE.

Proof: Without loss of generality, we use the "bean-bowl" system to illustrate our claim (shown in Fig. 9). In this dynamic system, the position and velocity of the bean can be treated as the state of the system, and the bowl is regarded as some constraints formed by the environment. Based on these assumptions, the state of the "bean-bowl" system at time t can be defined by the

$$\begin{cases} \dot{x}_1(t) = x_2(t) \\ \dot{x}_2(t) = M^{-1}(G + N(x_1, x_2, G) + f(x_1, x_2, N)) \\ x_1(t) \in \Omega. \end{cases} \tag{5}$$

where M is the inertia mass matrix, and Ω is the allowable region of the bean formed by the bowl. Specifically, the first equation describes the velocity-like state $x_2(t)$, which is the derivative of the position-like state $x_1(t)$. The second equation defines the acceleration-like state $\dot{x}_2(t)$ or $\ddot{x}_1(t)$, based on three kinds of forces acting on the bean, which are the gravity G, the supporting force of the bowl N, and the friction force f (shown in Fig. 9).

Moreover, in order to evaluate the stability of the system, we design a function $E(t)$ for the "bean-bowl" system as

$$E(t) = -Gx_1(t) + \frac{1}{2}Mx_2^2(t)$$

where Gx_1 denotes the potential energy and $\frac{1}{2}Mx_2{}^2$ is the kinetic energy. Obviously, the derivative of E is

$$\frac{\mathrm{d}E}{\mathrm{d}t} = -Gx_2 + \dot{x}_2 M x_2.$$

Similarly, to the case with the bean falling to the bowl, we can consider three situations of the state point in the bowl-like region, which are analyzed, respectively, as follows.

1) Case A (The State Point x_1 is on the Internal Surface of the Bowl-Like Region): As shown in Fig. 10(a), we set up a coordinate frame for the "bean-bowl" system, in which the base point is the lowest state point x_0 of the system, the *XOY*-plane is the tangent plane across x_0, and the *Z*-axis is perpendicular to the *XOY*-plane, pointing to the opening face of the bowl-like region.

Then, we have $x_1 > 0$ according to the *Z*-axis, and the angle between the directions of x_1 and the gravity G is larger than $90°$. Hence, $Gx_1 < 0$ and $E = -Gx_1 + \frac{1}{2}Mx_2^2 > 0$.

Moreover, the derivative of E can be calculated as

$$\begin{aligned} \frac{\mathrm{d}E}{\mathrm{d}t} &= -Gx_2 + \dot{x}_2 M x_2 \\ &= (-G + \dot{x}_2 M)\, x_2 \\ &= (N + f)\, x_2. \end{aligned}$$

When the state point is moving on the surface of the bowl-like region, the supporting force N is perpendicular to x_2 and the friction force f is opposite to x_2. Therefore, we have $\mathrm{d}E/\mathrm{d}t < 0$.

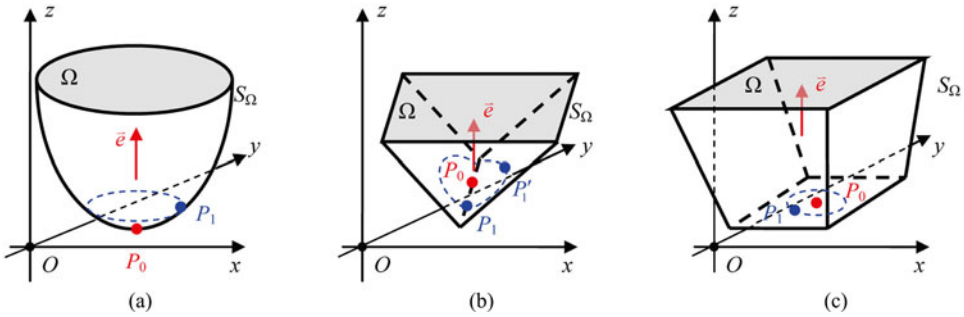

Fig. 12. Three examples of the stable points in different regions. Specifically, the point P_0 is a strictly stable point in (a), and is a stable one in (b) and (c).

It should be noted that the friction force f should be smaller than the resultant force G_f derived from G and N; otherwise, the state point will not move along the direction of G_f. On the other hand, f should be larger than zero, which is the precondition of $\mathrm{d}E/\mathrm{d}t < 0$.

2) Case B (The State Point x_1 is in the Inner Space of the Bowl-Like Region): In this situation, the initial state point x_1 is suspended on the inner space of Ω, without any contact with the surface of the region. As shown in Fig. 10(b), we also build up a similar coordinate system to the one introduced in the case A above.

Similarly, we can obtain that the energy $E > 0$ of the system and the supporting force $N = 0$. Moreover, the friction force f would be much smaller than that of the surface of the region. If it exists, the system will satisfy that $\mathrm{d}E/\mathrm{d}t = fx_2 < 0$. This situation will be further reduced to Case A, when the state point x_1 falls to the surface of the region under the effect of G.

3) Case C (The State Point x_1 is the Lowest Point x_0 of the Region): In this situation, the system state is passing through or staying at the lowest point x_0. We can easily obtain that at $x_1 = x_0 = 0$. As shown in Fig. 10(c), if the velocity-like state $x_2 > 0$, the system energy $E = \frac{1}{2}Mx_2^2 > 0$ and satisfies that $\mathrm{d}E/\mathrm{d}t = (N + f)x_2 < 0$. If $x_2 = 0$, we can obtain that $E = 0$ and $\mathrm{d}E/\mathrm{d}t = 0$; in the other word, the system state is stable at the point x_0.

Based on the analysis above, we can verify that $E \geq 0$ and specifically

$$\begin{cases} E\left(x_1(t), x_2(t)\right) = 0, & \text{when } x_1 = x_0 \text{and } x_2 = 0 \\ E\left(x_1(t), x_2(t)\right) > 0, & \text{otherwise} \end{cases}$$

and $\mathrm{d}E/\mathrm{d}t < 0$.

Therefore, the function $E\left(x_1(t), x_2(t)\right)$ is a Lyapunov function with a stable state x_0. The gravity G can be seen as the system input which is time-independent. According to Definition 1, this bowl-like region is an ARIE.

In addition to the bowl-like region, we now consider other kinds of regions which can also be regarded as attractive regions.

Theorem 2: The constrained domain is an ARIE if it is convex.

Proof: Corresponding to the definition above, we use Ω to denote the convex domain constrained by a time-continuous system, and S_Ω to represent the surface of Ω. Furthermore, we can define a system state $x_P(t)$, $x_P \in \Omega$ corresponding to an arbitrary point P in Ω.

First, we aim to find the lowest point P_s of the constrained domain, which can be further defined as the point with smallest system energy. According to the properties of the convex domain, P_s can be determined in different ways.

1) If S_Ω is smooth, an arbitrary point P on S_Ω will be a local minimum on the direction of its unit vector, due to the local curvature of the surface. Since Ω is convex, we can also obtain that P is the only global minimum on the direction of its unit vector. Therefore, any point on S_Ω can be selected as the lowest point P_s of the constrained domain. We can build up the coordinate frame for the convex domain, in which the base point is the lowest point P_s, the *XOY*-plane is the tangent plane $t(P_s)$ across P_s, and the *Z*-axis is along the direction of the unit vector of P_s [see Fig. 11(a)].
2) If S_Ω has one or more vertices, we also use P to denote one of the vertices on S_Ω. The tangent plane $t(P)$ across the point can be defined as one of the "subtangent planes" of P. Then, P is the local minimum on the direction of the unit vector of $t(P)$. Since Ω is convex, P is also the only global minimum on this direction. Hence, we can select any vertex of S_Ω to be the lowest point P_s of the constrained domain. Similarly, we can define the coordinate frame for the convex domain with vertices, as illustrated in Fig. 11(b).

Then, based on the defined lowest point P_s of the constrained domain, we can design an input $u(t)$ which is perpendicular to the tangent plane $t(P_s)$ and points to P_s. Therefore, the energy function $E\left(x_P(t)\right)$ of the system for an arbitrary point P on S_Ω can be defined as

$$E\left(x_P(t)\right) = -ux_P + \frac{1}{2}M\dot{x}_P^2$$

where M is the inertia mass matrix and $\dot{x}_P$ is the derivative of x_P, denoting the velocity-like state.

Finally, we prove that the function $E\left(x_P(t)\right)$ is a Lyapunov function with the stable state x_{Ps} corresponding to P_s. As illustrated in Fig. 11, the base point of the coordinates is the lowest point P_s. Therefore, we can obtain that $x_P \geq 0$ and $x_{Ps} = 0$. Furthermore, it is clear that $-ux_P \geq 0$ and $\frac{1}{2}M\dot{x}_P^2 \geq 0$. Hence,

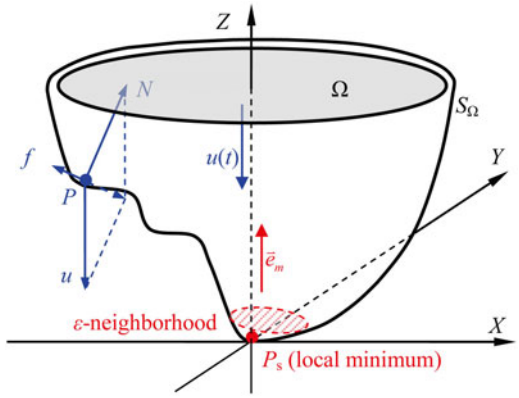

Fig. 13. Coordinate frame built up for the nonconvex domain Ω in which the Z-axis is along with the direction of $\vec{e}_m$ and P_s is the only one minimum in this direction, which is also a strictly stable point.

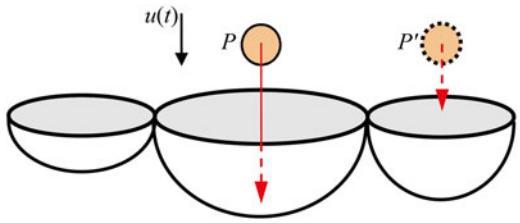

Fig. 14. Constrained domain with more than one stable points in the direction along $u(t)$ is not an attractive region. The system cannot converge to a global stable state from an arbitrary initial state under the effect of $u(t)$.

the energy function satisfies that

$$\begin{cases} E\left(x_P\right) = 0, & \text{when } x_P = x_{Ps} \text{ and } \dot{x}_P = 0 \\ E\left(x_P\right) > 0, & \text{otherwise.} \end{cases}$$

The derivative of $E\left(x_P(t)\right)$ can be calculated as

$$\frac{\mathrm{d}E}{\mathrm{d}t} = -u\dot{x}_P + \ddot{x}_P M \dot{x}_P = (N+f)\,\dot{x}_P.$$

Because the directions of the supporting force N and the friction force f are perpendicular and opposite to that of $\dot{x}_P$, we can obtain that $N\dot{x}_P = 0$ and $f\dot{x}_P < 0$. Therefore, the derivative of E satisfies that $\mathrm{d}E/\mathrm{d}t < 0$.

Based on the analysis above, it is clear that if the constrained domain is convex, then there must be a global lowest point P_s and its corresponding state-independent input $u(t)$, which can make the system converge to the stable state x_{Ps}. Under this circumstance, the constrained domain formed by the system is an attractive region.

On the other hand, the constrained domain may also be an attractive region even in the case when it is not convex, as stated in Theorem 3.

From the proof of Theorems 1 and 2, we can see that it is very important to determine a lowest state point in the constrained region. Then, based on this lowest point, we can design a state-independent input to promote the system state, which will finally converge at the lowest point. For a convex constrained region, it is easy to find this lowest point, which is actually the global minimum of this region in a certain direction. However, such a point cannot be simply assured for a nonconvex constrained region since in some directions, there may be several local minima which will attract the system state to converge to.

Thus, we introduce the concept of "stable point," which will help to further analyze the identification of the attractive region for a nonconvex constrained domain.

Definition 2: Assume that there is a constrained region Ω with a smooth boundary surface S_Ω. Then we can set up a coordinate system for Ω, in which the base point is O.

1) If there exist a point $P_0 \in S_\Omega$ and a unit vector $\vec{e}$ such that for an arbitrary point $P_1 \in S_\Omega$ with $\|P_1 - P_0\| < \epsilon$, where ϵ is an arbitrary real number, we have $\vec{e} \cdot \overrightarrow{OP_0} \leq \vec{e} \cdot \overrightarrow{OP_1}$, then we call P_0 the *stable point* in Ω at the direction of $\vec{e}$.
2) If P_0 satisfies that for the arbitrary point $P_1 \in S_\Omega$ with $\|P_1 - P_0\| < \epsilon$, we have $\vec{e} \cdot \overrightarrow{OP_0} < \vec{e} \cdot \overrightarrow{OP_1}$, then we call P_0 the *strictly stable point* in Ω at the direction of $\vec{e}$.

In Fig. 12, we use three simple examples to illustrate the stable points in different regions and the difference between the stable point and the strictly stable point. Obviously, the point P_0 in Fig. 12(a) strictly satisfies that $\vec{e} \cdot \overrightarrow{OP_0} < \vec{e} \cdot \overrightarrow{OP_1}$. Therefore, it is a strictly stable point with the direction of $\vec{e}$. In comparison, the neighboring points of P_0 in Fig. 12(b) can be divided into two classes: the points on the line across P_0 and perpendicular to $\vec{e}$, and others on S_Ω such as P_1 and P_1'. Due to the fact that $\vec{e} \cdot \overrightarrow{OP_0} = \vec{e} \cdot \overrightarrow{OP_1}$ and $\vec{e} \cdot \overrightarrow{OP_0} < \vec{e} \cdot \overrightarrow{OP_1'}$, P_0 is a stable point. In the more extreme situation, S_Ω has a flat plane perpendicular to $\vec{e}$, on which P_0 lies [see Fig. 12(c)]. Then, every point P_1 on this plane satisfies that $\vec{e} \cdot \overrightarrow{OP_0} = \vec{e} \cdot \overrightarrow{OP_1}$, so P_0 is also a stable point. These examples also remind us that the stable point is not the only one in many situations, even in a small neighborhood of the region.

It should be noted that the definition of stable point is not equal to that of local minimum. As shown in Fig. 12(b) and (c), there is no any local minimum in the built coordinate frame, but there are infinitely many stable points, whose correspondent system states can shift in their neighborhood freely. Therefore, the constrained regions in Fig. 12(b) and (c) are not ARIEs apparently.

Based on the concept of the "stable point," we can further identify whether or not a constrained region is an ARIE in a more general situation, such as a nonconvex constrained region.

Theorem 3: A nonconvex domain can be an attractive region if there exists *only one* stable point along some direction which is a strictly stable point.

Proof: As shown in Fig. 13, the constrained domain Ω is nonconvex. The surface of Ω is denoted by S_Ω. In some directions, there are several stable points which may attract the state system to converge to. However, along the direction of a certain unit vector $\vec{e}_m$, S_Ω has the only one stable point P_s, which is corresponding to the system state x_0.

Then, we can set up the coordinate frame, which satisfies that P_s is the base point and Z-axis is along with the direction of $\vec{e}_m$. According to the definition of strictly stable points, P_s is the only one local minimum in the ϵ-neighborhood region of P_s. Since P_s is also the only one stable point in the direction

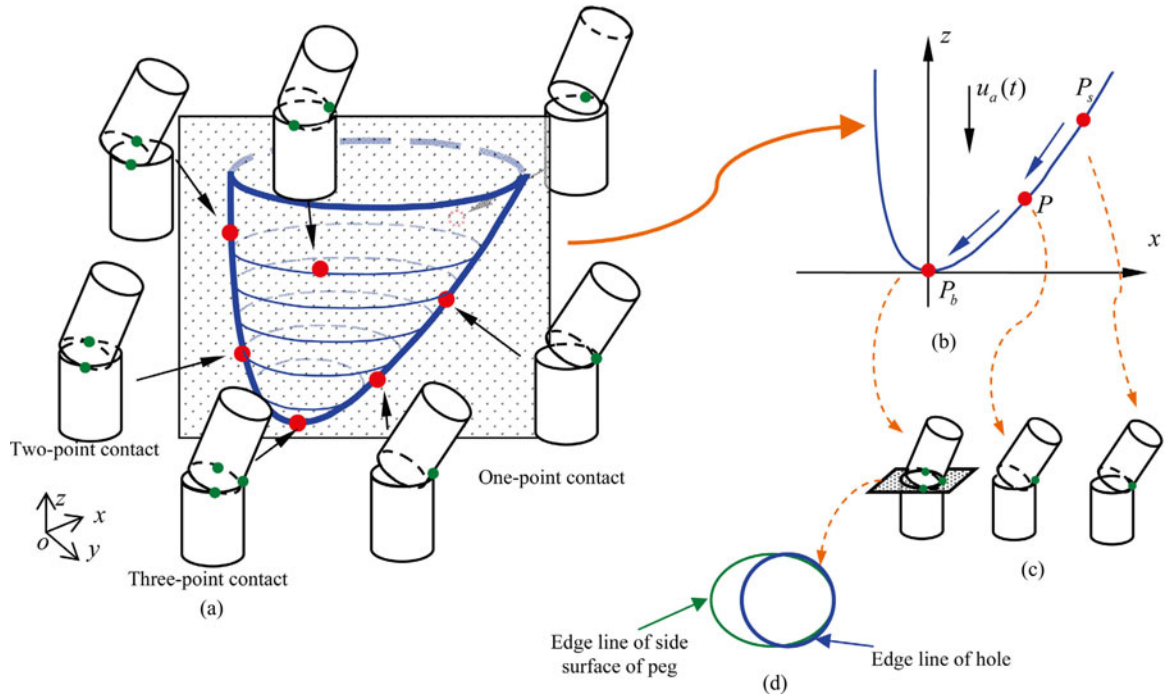

Fig. 15. Correspondence between the physical states and the points in the attractive region formed by shaft-hole assembly. In (a), the red points on the surface of the constrained region denote the contact states illustrated by the subfigures nearby. Green points are the contact points between the peg and hole. (b) Curve on the attractive region cutting by the *XOZ*-plane. (c) Corresponding change of the physical state, and (d) shows the projection on the *XOY*-plane of the edge of the hole and peg, respectively.

of $\vec{e}_m$, there will not be any other local minimum on S_Ω in this direction. Therefore, P_s is the global minimum of S_Ω along the direction of $\vec{e}_m$.

For the system with the constrained region Ω, we further define the energy function $E(x_P(t))$ as

$$E(x_P(t)) = -ux_P + \frac{1}{2}M\dot{x}_P^2$$

where x_P is the system state corresponding to an arbitrary point $P \in \Omega$. Moreover, $u(t)$ is the system input with the direction opposite to that of $\vec{e}_m$, which can be described as

$$u(t) = -U \cdot \vec{e}_m$$

where U is a positive real number.

Similar to Theorem 2, we can prove that the function $E(x_P(t))$ is a Lyapunov function with the stable state x_0 corresponding to P_s. Obviously, in the coordinate frame illustrated in Fig. 13, we have $-ux_P \geq 0$, and this equation will be true when $x_P = x_0$. Therefore, the energy function E satisfies that $E(x_P(t)) = -ux_P + \frac{1}{2}M\dot{x}_P^2 \geq 0$, and the equation will be true when $x_P = x_0$ and $\dot{x}_P = 0$. The derivative of E can be calculated as

$$\frac{\mathrm{d}E}{\mathrm{d}t} = -u\dot{x}_P + \ddot{x}_P M\dot{x}_P = (N+f)\,\dot{x}_P.$$

Due to the fact that the directions of the supporting force N and the friction force f are perpendicular to and opposite to that of $\dot{x}_P$, we can obtain that $\mathrm{d}E/\mathrm{d}t = f\dot{x}_P < 0$.

Based on the analysis above, the nonconvex constrained domain can be an attractive region if there is only one stable point P_s which is also a strictly stable point, along some direction

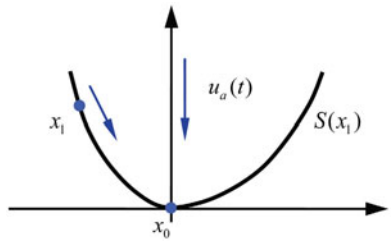

Fig. 16. "Boundary of the attractive region" $S(x)$ has the equilibrium point x_0 in the attractive region.

such as that of $\vec{e}_m$. We can design a state-independent input $u(t)$ opposite to $\vec{e}_m$ so that the system will converge to the stable state x_0 corresponding to P_s.

Theorem 4: A constrained region is not an attractive region if the region has more than one stable points in the direction of any input.

As shown in Fig. 14, this region is clearly not convex since it has more than one stable points along the input direction. For any input, the system cannot converge to a global stable state. Therefore, the constrained region of this system is not an ARIE. It should be noted that, in such a case, we may find more than one attractive regions, which can also be used for manipulation design, such as the example on 3-D object localization in Section II-C. This will be further discussed in our future work.

C. Correspondence Between the Physical States and the Points in the Attractive Region

We further analyze the relationship between the physical state and the point in the attractive region, which help to make a

strategy in the practical manipulation. For a general ARIE formed by industrial manipulation, according to the theorems above, the points on the attractive region have explicit correspondences to the system states in the physical manipulation space. We take the round-peg-hole insertion as an example to explain this kind of relationship. As shown in Fig. 15(a), the attractive region is with the *OXYZ* coordinate frame, where the base point is the stable point of the attractive region, the *XOY*-plane is the upper-surface of the hole, and the *XOZ*-plane is parallel to the peg's projection on the *XOY*-plane.

1) Using a Plane Parallel to the XOY-Plane to Crosscut the Attractive Region: A closed curve will be obtained on this plane. The shape of this curve is related to some boundary edges of the hole. If we use the upper surface of the attractive region for this crosscutting, the points on the obtained curve would be the changing positions of the peg's lower end, which are corresponding to the states with one-point contact between the shaft's lower end and hole's boundary.

2) Using the XOZ-Plane to cut the Attractive Region Vertically: A convex curve would be obtained. As shown in Fig. 15(b), this curve is divided into two parts by the base point.

The point on the right half part of the curve denotes the inserted depth related to the peg's movement along the *x*-axis, which is corresponding to the state of one-point contact on the peg's side surface. As shown in Fig. 15(c), when the position of the peg's lower end is moving along the *x*-axis, the one-point contact state is changing along with the inserted depth and finally reaches the three-point contact state. This process is corresponding to the trajectory from P_s to P_b on the curve. Hence, the shape of the right part of the curve is related to the property of the peg's side surface.

The points on the left half part of the curve formed by the cutting of the *XOZ*-plane also denote the depths of the peg in hole with different coordinates on the *x*-axis. But these points are corresponding to the states of a two-point contact on the peg's lower surface. Therefore, the curve shape is related to the property of the peg's lower surface.

For a more general consideration, the right half part of the curved surface of the attractive region can be seen as the accumulation of the 2-D cutting curves series, and therefore, it reflects the shape of the hole's right boundary and the peg's side surface. Similarly, the left half part of the curved surface reflects the shape of the hole's left boundary and the peg's lower surface.

Furthermore, we can imagine that a series of 2-D attractive regions can be obtained based on cutting a 3-D attractive region along a certain direction. As mentioned above, the relationship between the points in the attractive region and the physical states can be easily analyzed based on these 2-D attractive regions. Moreover, the properties of the original 3-D attractive region are inherited by these 2D ones. Therefore, when we are solving a high-dimensional and complex attractive region, similar cutting procedure can be applied for the analysis. The physical meaning of the points in the configuration space will be obtained more clearly based on the low-dimensional attractive regions. Hence, this processing is very significant to the high-precision manipulation for practical application. We will discuss this mechanism in the next section.

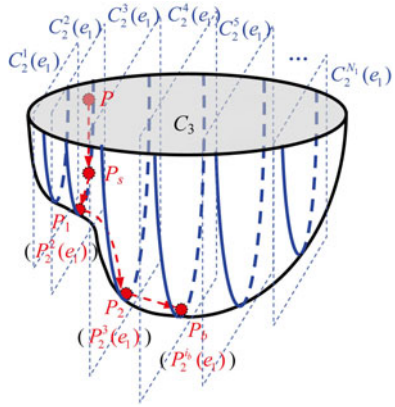

Fig. 17. Attractive region C_3 in 3-D with its 2-D cut profiles, which are also attractive regions. An arbitrary point P in the constrained region can fall to the point P_s on the surface, then converge to the stable point on the own cut profile, at last transfer to the lowest point P_b of C_3.

IV. Extension of Attractive Regions in Higher Dimensional Spaces

In the previous discussion, we mainly focused on the visible attractive region in a three or less dimensional configuration space and the association with physical states. However, the constrained region of most manipulation systems could be constructed in a higher dimensional configuration space.

Therefore, we will further extend the concept of ARIE to the configuration space in $\mathbb{R}^n$ in this section. First, we introduce the method of identification of the attractive region in a high-dimensional configuration space, and then an analysis is given to show the relationship between the attractive regions in the high- and low-dimensional spaces.

A. Generalization of the Concept of ARIE to a High-Dimensional Configuration Space

The generalization of the concept of ARIE can be discussed from three different aspects: The general formulation in the $\mathbb{R}^n$ configuration space, the relationship in different dimensions, and the convex properties of the attractive region.

Without loss of generality, we may consider the following nonlinear system

$$\begin{cases} \dot{x}_1 = x_2 \\ \dot{x}_2 = f(x_1 + u_a(t) + u_p(x_1, t)) \\ x_1 \in \Omega \end{cases} \tag{6}$$

where $x_1(t)$ and $x_2(t)$ denote the position-like state and the velocity-like state, respectively, u_a is the state-independent input of the system, and u_p is the passive, state-dependent input formed by the constraints of the environment. It should be noted that the state $x_1(t)$ is always in the constrained region Ω. If we can find such an input $u_a(t)$ under which the system will finally converge to a stable state, the region Ω will form an ARIE.

Based on the definition of ARIE, we will discuss conditions for the existence of attractive regions in the configuration space with respect to the nonlinear system defined by (6).

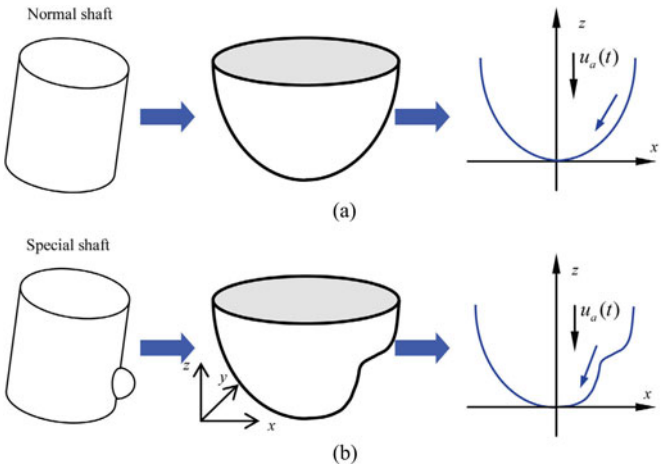

Fig. 18. Attractive region formed by assembly of the hole and different shafts, (a) the normal one (b) and the special one with a prominence on side.

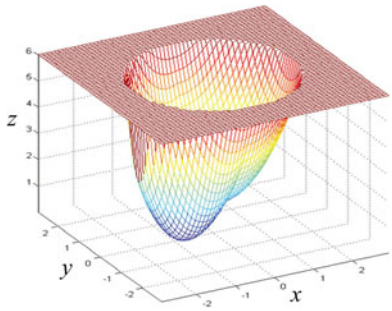

Fig. 19. Simulation of the attractive region formed by the insertion of specific shaft and hole. The radii of the hole and the shaft's prominence are 3 and 0.2 unit length, respectively.

Without loss of generality, we assume that $S(x_1)$ is the boundary of the system defined by (6) and x_0 is the only stable state of the system. For any initial state x_1, if there exists a path along the boundary of the system leading x_1 to x_0, then an attractive region exists in the configuration space of the system.

Theorem 5: A constrained region Ω with its boundary $S(x_1)$ in the configuration space formed by a nonlinear system is an attractive region if for any state x_1, the following conditions are satisfied:

$$\begin{cases} S(x_1) = S(x_0), & \text{when } x_1 = x_0 \\ S(x_1) > S(x_0) & \forall x_1 \in \Omega \backslash \{x_0\} \\ \frac{\mathrm{d}^2 S(x_1)}{\mathrm{d}{x_1}^2} > 0 & \forall x_1 \in \Omega \backslash \{x_0\}. \end{cases} \tag{7}$$

Proof: Without loss of generality, we assume that x_0 is an arbitrary point on the boundary $S(x_1)$, $u(t)$ is an state-independent input toward the state x_0, and $l(x_1)$ is the moving curve of the system state on the boundary $S(x_1)$ under the effect of the input $u(t)$. According to (7), the system state x_1 tends to x_0 with the time passing. Thus, $l(x_1)$ satisfies that

$$\begin{cases} l(x_1) > S(x_0), & \text{when } x_1 \in \Omega \backslash \{x_0\} \\ l(x_1) = S(x_1), & \text{when } x_1 = x_0 \\ \frac{\mathrm{d}l(x_1,t)}{\mathrm{d}t} = \frac{\mathrm{d}l(x_1,t)}{\mathrm{d}x_1(t)} \times \frac{\mathrm{d}x_1(t)}{\mathrm{d}t} < 0 \end{cases}.$$

The third inequality is true since

$$\begin{cases} x_1 < x_0, \frac{\mathrm{d}^2 S(x_1)}{\mathrm{d}{x_1}^2} > 0 \Rightarrow \frac{\mathrm{d}x_1(t)}{\mathrm{d}t} > 0, & \frac{\mathrm{d}l(x_1,t)}{\mathrm{d}x_1(t)} < 0 \\ x_1 > x_0, \frac{\mathrm{d}^2 S(x_1)}{\mathrm{d}{x_1}^2} > 0 \Rightarrow \frac{\mathrm{d}x_1(t)}{\mathrm{d}t} < 0, & \frac{\mathrm{d}l(x_1,t)}{\mathrm{d}x_1(t)} > 0 \end{cases}.$$

Let $V(y) = V(x_1 - x_0) = l(x_1) - S(x_0)$. Then, it is satisfied that $V(0) = 0$ and $V(y) > 0$, $y \in Y \backslash \{0\}$, where Y is a neighborhood region around $y = 0$, that is, $Y = \{x_1 - x_0 | x_1 \in \Omega\}$. Therefore, $V(y)$ is a Lyapunov function, and $y = 0$ is an equilibrium point of the region Y; in other words, the system $S(x_1)$ has an equilibrium point $x_1 = x_0$ in the region Ω.

In Theorem 5, $S(x_1)$ is called "the boundary of the attractive region." For generalization, the boundary $S(x_1)$ in the coordinate frame shown in Fig. 16, satisfies that

$$\begin{cases} S(x_1) = 0, & \text{when } x_1 = x_0 \\ S(x_1) > 0, & \text{when } x_1 \in \Omega \backslash \{x_0\} \\ \frac{\mathrm{d}S(x_1(t))}{\mathrm{d}t} < 0, & x_1 \in \Omega \backslash \{x_0\} \end{cases}. \tag{8}$$

It represents some kind of "energy" of the system. Under a certain input, the "energy" of the system is reduced with time t passing and the system will finally approach to the stable state. Correspondingly, if we find a state-independent input $u(t)$, the system will be "pushed" into the stable state. From this point of view, the Lyapunov function is useful in constructing the state-independent input for the ARIE.

In general, designing a robotic strategy in a very high-dimensional space is difficult. In comparison, converting this high-dimensional problem into a set of low-dimensional ones can be a more effective way to solve the problem. Such an example is detailed below.

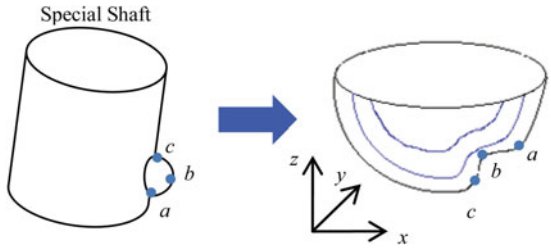

Fig. 20. States with specifically contact point (marked by blue color) between the shaft and the hole in the physical space and the correspondent points in the attractive region.

B. Relationship of the Attractive Regions in Different Dimensions

In this section, we will visualize the high-dimensional attractive region by establishing the mapping from a high-dimensional space to its subspaces.

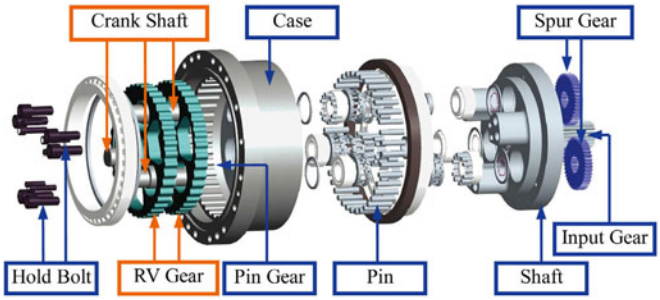

Fig. 21. Main components of RV reducer.

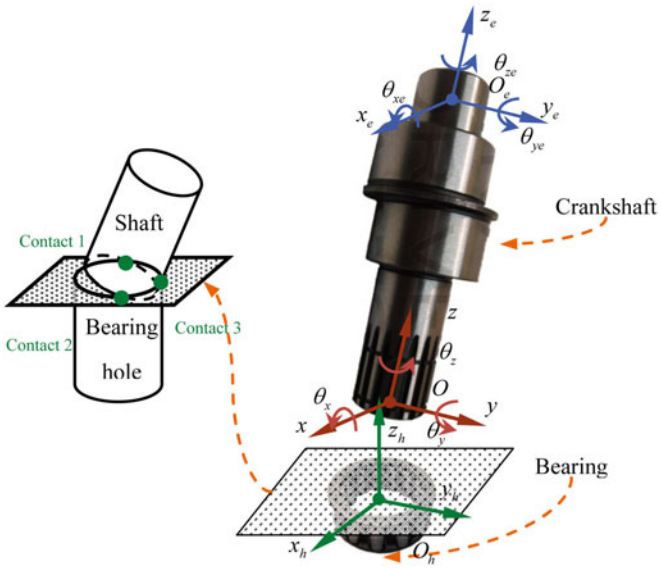

Fig. 22. Crankshaft-bearing insertion and the built coordinate frames based on three different base points, including the center of bearing hole, the bottom, and the top end of crankshaft. The left figure denotes the stable state with three points contacted between the crankshaft and bearing.

We mainly consider the relationship between a 3-D attractive region and 2-D attractive regions for illustration. Assume that a nonlinear system in $\mathbb{R}^3$ as follows:

$$\begin{cases} \dot{x} = f\left(x, u_a(t), u_p(x,t)\right) \\ x \in C_3 \end{cases} \tag{9}$$

where x is the state of the system, C_3 is the boundary of the constrained region of the system in $\mathbb{R}^3$, u_a is the state-independent input of the system, and u_p is the passive, state-dependent input. We have the following result that cutting a 3-D surface at a certain direction from continuous changing positions will form a cluster of 2-D cut profiles of the 3-D region. We can further derive the conclusion as below.

Theorem 6: If there exist a cluster of 2-D cut profiles, each of which is an attractive region, and the region formed by the stable points of the cluster of cut profiles is also an attractive region, then the corresponding domain C_3 forms an attractive region in $\mathbb{R}^3$.

Proof: Denote by $C_2(e_k)$, $k = 1, 2, \ldots, N$, the cluster of profiles in $\mathbb{R}^2$ formed by cutting C_3 from the direction e_k. Then, based on $C_2^i(e_k), i = 1, 2, \ldots, N_k$, which is the i-th constrained

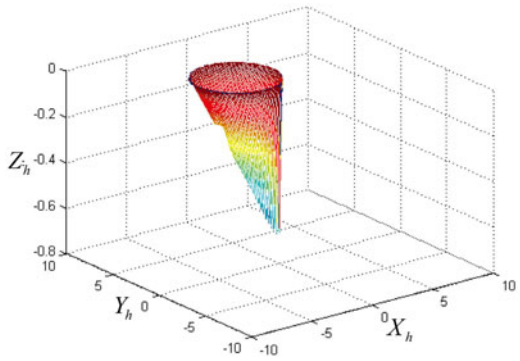

Fig. 23. Simulation of the crankshaft position $h = G(p)$ with fixed $[\theta_x, \theta_y, \theta_z]$. The attractive region is formed by the environment constraint when the crankshaft bottom is moving on the $X_h Y_h$ plane. Radius of the bearing hole is set to be 3 unit length.

region of each cut profile in the set $C_2(e_k)$, we can obtain that

$$C_3 = \bigcup_{i=1}^{N_1} C_2^i(e_1) = \bigcup_{i=1}^{N_2} C_2^i(e_2) = \cdots = \bigcup_{i=1}^{N_k} C_2^i(e_k).$$

Without loss of generality, we assume that each profile in the set $C_2(e_1)$ is an attractive region, that is, $C_2^i(e_1) \in \Omega_2$, where Ω_2 denotes the 2-D attractive region set. The bottom of the attractive region $C_2^i(e_1)$ is supposed to be $P_2^i(e_1)$. From the condition that the region formed by the stable points of the cluster of the cut profiles is also an attractive region, we obtain that

$$\begin{cases} \bigcup_{i=1}^{N_1} P_2^i(e_1) \in \Omega_2 \\ P_2^i(e_1) \to P_2^{i_b}(e_1) = P_b \end{cases} \tag{10}$$

where P_b is the equilibrium point of this attractive region.

In the following, we will prove that an arbitrary point P inside the constrained region C_3 will converge to the unique stable point P_b. Obviously, any inner point P will first fall onto the surface of C_3, where its corresponding surface point is assumed to be P_s. We have

$$P_s \in \bigcup_{i=1}^{N_1} C_2^i(e_1) \Rightarrow P_s \in C_2^{i_s}(e_1).$$

Under the effect of the input $u(t)$, P_s will transfer to a new point P_1, which is the stable point of the 2-D profile $C_2^{i_s}(e_1)$, that is, $P_1 = P_2^{i_s}(e_1)$. According to (10), $\bigcup_{i=1}^{N_1} P_2^i(e_1)$ is also an attractive region in Ω_2. Therefore, P_1 will transfer to P_2, to P_3, and so on (see Fig. 17).

The surface point P_s will finally achieve some stable state $P_n = P_2^{i_n}(e_1)$. From (10), we obtain that $P_2^{i_n}(e_1) \to P_2^{i_b}(e_1) = P_b$ and C_3 is an ARIE.

Due to the fact that the constrained region formed by most mechanical systems is in a three- or higher dimensional configuration space, the decomposition method mentioned above is an effective way to construct a set of attractive regions with a low dimensionality, which are significant for practical manufacturing.

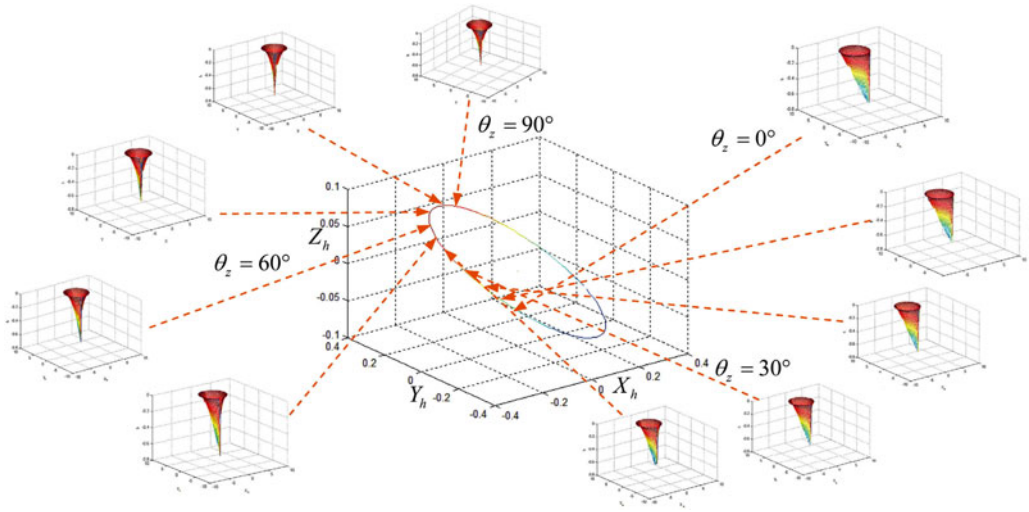

Fig. 24. Simulation results of $h = G(p'_e)$ with $p'_e = [x_{e-h}, y_{e-h}, z_{e-h}, \theta_{xe}, \theta_{ye}, \theta_z]^T$. The movement of the crankshaft top end center forms an ellipse in the $X_h Y_h Z_h$ space. The figures denote the formed attractive regions corresponding to the points on the elliptical trajectory. Eccentricity of the crankshaft is 0.3 unit length.

V. Application of the Attractive Regions in Industrial Manufacturing

As described in Section II, we have found that the attractive region widely exists in the configuration space of manufacturing systems. The theoretical foundation of the concept of ARIE is provided for more general situations in Sections III and IV, compared with our previous work. In this respect, we discuss the implementation of some typical manipulation tasks based on this theory to show the application significance of the proposed work. This evaluation is carried out from two perspectives: The nonideal configuration space in general manipulation and the high-dimensional one in a challenging task.

A. Implementation Based on Nonbowl-Like Attractive Regions

As mentioned in Section III-C, for the attractive region formed by the peg-hole insertion, we find that part of the attractive region's boundary is related to the shape of peg's side surface, which affects the distance between the peg and hole on the vertical axis. If the property of the peg's side surface is changed, such as adding a spherical prominence which is a common situation with machining error, the mapping between the inserted depth and the x-axis coordinate will change.

As shown in Fig. 18, let the peg move along the x-axis, when the contact on the side surface reaches the bottom of the prominence, longer distance of the movement on the x-axis will be needed for the same inserted depth compared with general insertion. This is because the curved surface of the prominence changed the original slope of peg's side. Reflected on the attractive region (see Fig. 19) formed by the inserted depth and the peg's movement, the curve of the boundary is plicate on the z-axis. Similarly, the top side of prominence will also change the boundary shape of the attractive region.

Therefore, when this kind of attractive regions is obtained, we can confirm that there must be some defect or special designing on the shaft side surface. Similarly, more conclusion can be obtained based on analyzing the boundary shape of the attractive region. If the shape of the upper boundary of the hole is changed, the closed curve on the crosscutting plane of the attractive region will change. If the shape of the peg's lower end is changed, the shape of one side boundary of the attractive region will change, just like the influence on the other side boundary from the peg's side surface.

Although the attractive region influenced by the deformation of the peg and hole is not a standard one, we can still analyze the cause of the deformation based on the correspondence between the physical state and the point on the boundary curve and adjust the assembly strategy appropriately to handle the insertion.

We take the peg and hole with defect on the side surface as an example to illustrate the manipulation based on a nonbowl-like attractive region. As mentioned above, the attractive region formed by this system is not a standard one, whose boundary of one side is plicate along the z-axis. We can still solve the insertion problem by adjusting the rotation angles θ_x and θ_y appropriately.

As the normal insertion based on the attractive region, the peg should reach the one-point contact state. As shown in Fig. 20, if the touching point of the hole is on the *a*-*b* curve, the inserted depth will be reduced by the surface of prominence. In this situation, we can use a smaller inclined angle of the peg to smoothen the movement on the z-axis. If the touching point is on the *b*-*c* curve, the inserted depth will change quickly along the peg's movement on the x-axis (like jumping). Then, we should enlarge the inclined angle to reduce the insertion speed. We can build up a mapping between the inclined angle (relating to the rotation angles θ_x and θ_y) and the peg's movement on the x-axis. The assembly strategy can be changed adaptively based on the mapping to reduce the influence of prominence.

B. Implementation of High-Dimensional Attractive Regions on Complex Tasks

As mentioned in Section IV, attractive regions with a high dimensionality widely exist in complex manipulation. One rep-

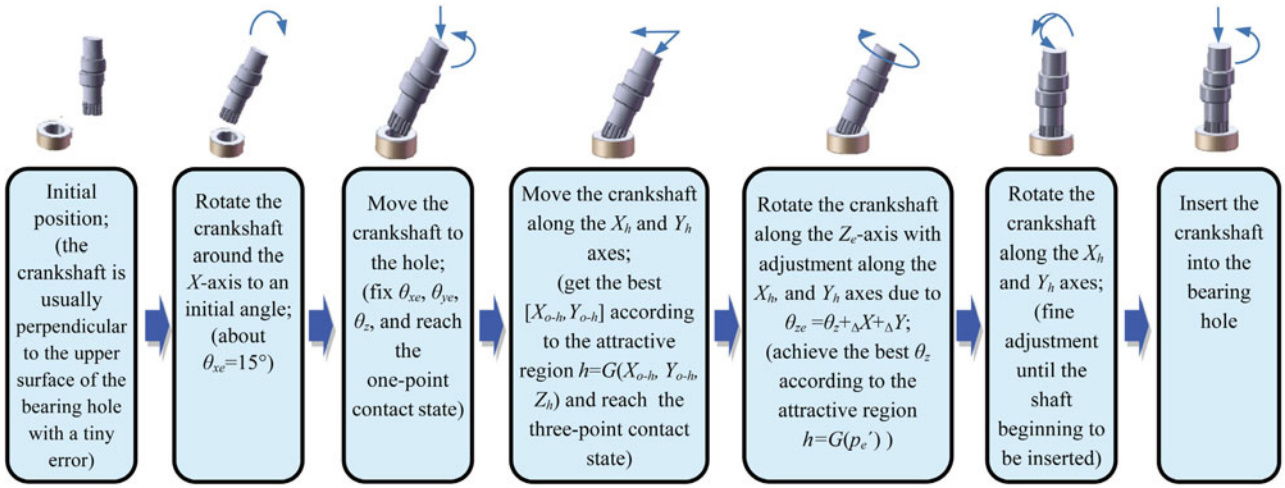

Fig. 25. Procedures of the implementation of crankshaft insertion.

resentative work is the manufacturing of Rot-Vector (RV) reducer, which is widely used in robotics system and is also a key task in the "04 Project" of the "China National Science and Technology Major Project."

As shown in Fig. 21, the RV reducer is with a structure of hollow shaft, whose implementation can be divided into a series of assembly subproblems. The key components of the RV reducer include 1) case, 2) shaft and hold flange, 3) three crankshafts along with their bearing packs, 4) a pair of RV gears, and 5) input and spur shafts. In the whole implementation, the crankshafts will be assembled in the bearing packs first. Then, the rotation angles of RV gears will be adjusted according to the holes on them for the insertion of crankshafts. At last, the hold flange and shaft will be assembled in the anomalous holes of RV gears, which is a typical multipeg-hole insertion. The main difficulty is the insertion of crankshaft, where the crankshaft's eccentricity enhances the implementation complexity. Compared with the normal peg-hole insertion, this problem requires a much higher precision of the system control method.

1) Analysis of the Attractive Region of Crankshaft-Hole Insertion in RV Reducer: We mainly focus on the analysis of ARIE existed in the crankshaft-hole insertion of RV reducer and its application to illustrate effectiveness of the proposed method.

We define the coordinate frames as below (see Fig. 22). The base coordinate frame $X_hY_hZ_h$ is fixed on the hole of RV gears. The base points of coordinates $X_eY_eZ_e$ and XYZ are corresponding to the positions of top and bottom end centers of the crankshaft, respectively. p and p_e are the coordinates of the two base points in $X_hY_hZ_h$. We use h to denote the crankshaft position on the Z_h axis, which can be described as

$$p = [x_{o-h}, y_{o-h}, z_{o-h}, \theta_x, \theta_y, \theta_z]^T \in \mathbb{R}^6 \text{ or}$$

$$p_e = [x_{e-h}, y_{e-h}, z_{e-h}, \theta_{xe}, \theta_{ye}, \theta_{ze}]^T \in \mathbb{R}^6$$
$$\text{and } h = G(p), \text{ or } h = G(p_e)$$

where x_{o-h}, y_{o-h} and z_{o-h} denote the deviation from the *XYZ* coordinate frame to the base coordinate frame $X_hY_hZ_h$, and x_{e-h}, y_{e-h}, z_{e-h} denote the deviation between the $X_eY_eZ_e$ and $X_hY_hZ_h$ coordinate frames. Similarly, θ_x, θ_y, and θ_z are the angular differences of the object rotation in the *XYZ* and $X_hY_hZ_h$ coordinate frames, respectively, and θ_{xe}, θ_{ye}, θ_{ze} are the angular differences of the object rotation in the $X_eY_eZ_e$ and $X_hY_hZ_h$ coordinate frames.

It should be noted that the relationship between $[\theta_x, \theta_y, \theta_z]$ and $[\theta_{xe}, \theta_{ye}, \theta_{ze}]$ is known, due to the structure information of the crankshaft. Hence, we can use $p = [x_{o-h}, y_{o-h}, z_{o-h}, \theta_x, \theta_y, \theta_z]^T \in \mathbb{R}^6$ to denote the crankshaft position as the alternative choice. If the rotation of crankshaft $[\theta_x, \theta_y, \theta_z]$ is fixed, the crankshaft motion under the constraint of RV gear hole can be described as $h = G([x_{o-h}, y_{o-h}, z_{o-h}]^T) \in R^3$. As illustrated in Fig. 23, the formed constrained region of this motion has similar characteristic to the attractive region of the typical shaft-hole insertion. It is also a classical attractive region due to the only one stable point.

The bottom part of the crankshaft is rotational symmetric about the *Z*-axis. Therefore, the position of crankshaft bottom end h is not changed by θ_z. However, due to the eccentricity, the crankshaft top end center $p_e = [x_{e-h}, y_{e-h}, z_{e-h}, \theta_{xe}, \theta_{ye}, \theta_{ze}]^T$ would change on the coordinates of X_h, Y_h, Z_h, and θ_{ze}. As shown in Fig. 24, we illustrate the changing trajectory of the position on the X_h, Y_h, and Z_h axes, which is an ellipse. Actually, this trajectory is in the 4-D space including θ_{ze} axis. We use the 3-D coordinates for clear illustration. If we assume that $\theta_{ze} = f(\theta_z)$, the center position $p_e = [x_{e-h}, y_{e-h}, z_{e-h}, \theta_{xe}, \theta_{ye}, f(\theta_z)]^T$ can be also wrote as $p'_e = [x_{e-h}, y_{e-h}, z_{e-h}, \theta_{xe}, \theta_{ye}, \theta_z]^T$. Let $[\theta_{xe}, \theta_{ye}]$ be fixed, and let $h = G(p'_e)$ change along the elliptical trajectory (θ_z is also changing correspondingly), we will obtain a series of constrained regions, which are all similar to the one in Fig. 23. The correspondences between the points on the trajectory and the constrained regions are shown in Fig. 24.

Based on the simulation and analysis above, we build up the implicit relationship between h and $p'_e = [x_{e-h}, y_{e-h}, z_{e-h}, \theta_{xe}, \theta_{ye}, \theta_z]^T$, which can be written as $h = G(p'_e)$. A series of attractive regions exist in this relationship, which can be used to calculate the lowest insertion point of the shaft in the crankshaft assembly. Actually, the lowest insertion

point is a stable state with three points contacted, which can be used to formulate the control strategy for the high-precision assembly.

2) Procedure of Assembly Strategy for the Crankshaft-Hole Insertion Based on the Attractive Region: In the practical manipulation, the robot gripper grips the upper end of the crankshaft and moves its position to realize the assembly of the crankshaft and RV gears. Specifically, we have found the relationship between h and $p'_e = [x_{e-h}, y_{e-h}, z_{e-h}, \theta_{xe}, \theta_{ye}, \theta_z]^T$ in the simulation. The suitable θ_z can be selected based on the relationship. When $[\theta_{xe}, \theta_{ye}, \theta_z]$ is fixed, the crankshaft position h will be reduced to a subproblem with a classical attractive region in the $[x_{e-h}, y_{e-h}, z_{e-h}]$ space, which is similar to the problem of a typical peg-hole insertion.

Hence, as the typical peg-hole insertion, the crankshaft assembly can be solved according to the substep control strategy of the robot gripper as following. First, we find the best inserted position $[x_{e-h}, y_{e-h}]$ on the $X_h Y_h$ plane based on the attractive region formed by h and $[x_{e-h}, y_{e-h}, z_{e-h}]$. The initial rotation angle $[\theta_{xe}, \theta_{ye}, \theta_z]$ of the crankshaft is selected artificially and fixed in this process. Then, when the system state of three-point contact between the crankshaft and bearing is reached, we calculate the best angle θ_z according to $h = G(p'_e)$, with which the shaft will have the global lowest insertion point. Correspondent rotating manipulation is made by the gripper based on the control strategy. At last, the crankshaft is rotated and inserted into the hole by the constraints from the changing of $[\theta_{xe}, \theta_{ye}]$. Fig. 25 also shows the implementation of crankshaft insertion in RV reducer.

VI. Future Work and Conclusion

In the configuration space of a dynamic system, we have found that the attractive region formed by the constraints of the environment widely exists, which can be used to eliminate the uncertainty of the system without sensor feedback.

Further, we have given a formal and generalized definition of the ARIE and the correspondent identification method in this paper. Compared with our previous work with simple and desired configuration spaces, the concept of ARIE can be extended to apply in systems with a more complex and nonideal configuration space. The experimental simulations showed that high-precision and high-reliability tasks without sensor information could be realized based on the proposed theoretical foundation of ARIE.

In the future, ARIE will be applied in assembly of car motors and reducers as well as in the design of grippers during the assembly process, which is in fact an ongoing project supported by an Intelligent Equipment Special Grant from the State Development and Reform Commission and the Special Program of Beijing Municipal Science and Technology Commission. We are currently testing the multipeg-hole and polygon-peg-hole insertions based on the concept of ARIE in collaboration with some automobile manufacturers. Moreover, we believe that the concept of the attractive region can be introduced to the dynamic control of robots [49] and the subspace learning theory. For example, it is found that there are some attractive regions in face recognition. Using these attractive regions, we can retrieve the frontal face image from an initial range of facial configurations.

Acknowledgment

The authors would like to thank the anonymous reviewers and technical editor for their helpful comments and suggestions. We also thank Prof. B. Zhang of AMSS, CAS for many enlightening discussions on ARIE, and for carefully polishing this paper.

References

[1] B. Baksys, J. Baskutien, A. B. Povilionis, and K. Ramanuskyte, "Sensorless vibratory manipulation of the automatically assembled parts," *Solid State Phenomena*, vol. 164, pp. 265–270, 2010.

[2] K. Sonoda and A. Shimada, "A joint angle sensorless grasping control on two-fingered robot hands," in *Proc. 11th IEEE Int. Workshop Adv. Motion Control*, 2010, pp. 774–779.

[3] S. M. Kristek and D. A. Shell, "Orienting deformable polygonal parts without sensors," in *Proc. IEEE/RSJ Int. Conf. Intell. Robots Syst.*, 2012, pp. 973–979.

[4] H. Qiao, "Attractive regions in the environment for motion planning," in *Proc. IEEE Int. Conf. Robot. Autom.*, 2000, vol. 2, pp. 1420–1427.

[5] H. Qiao, "Strategy investigation with generalized attractive regions," in *Proc. IEEE Int. Conf. Robot. Autom.*, 2002, vol. 3, pp. 3315–3320.

[6] H. Qiao, "Application of 'generalized attractive region' in orienting 3D polyhedral part," in *Proc. IEEE Int. Conf. Robot. Autom.*, 2003, vol. 2, pp. 2248–2254.

[7] J. H. Su, H. Qiao, C. K. Liu, and Z. C. Ou, "A new insertion strategy for a peg in an unfixed hole of the piston rod assembly," *Int. J. Adv. Manufac. Technol.*, vol. 59, pp. 1211–1225, 2012.

[8] J. H. Su, H. Qiao, and C. K. Liu, "A vision-based 3d grasp planning approach with one single image," in *Proc. IEEE Int. Conf. Mechatron. Autom.*, 2009, vols. 1–7, pp. 3281–3286.

[9] C. K. Liu, H. Qiao, and B. Zhang, "Stable sensorless localization of 3-D objects," *IEEE Trans. Syst., Man, Cybern. C, Appl. Rev.*, vol. 41, no. 6, pp. 923–941, Nov. 2011.

[10] H. Qiao and B. Zhang, "Combination of strategy investigation and utilization of sensor signals in robotic assembly," *Proc. Inst. Mech. Eng. B, J. Eng. Manuf.*, vol. 214, pp. 657–669, 2000.

[11] H. Inoue, "Force feedback in precise assembly tasks," *Bullet. Electrotechnical Lab.*, vol. 38, no. 12, pp. 775–789, 1974.

[12] T. Lozano-Perez and P. H. Winston, "LAMA: A language for automatic mechanical assembly," in *Proc. Int. Conf. Artif. Intell.*, 1977, pp. 710–716.

[13] F. Dietrich, D. Buchholz, F. Wobbe, F. Sowinski, A. Raatz, W. Schumacher, and F. M. Wahl, "On contact models for assembly tasks: Experimental investigation beyond the peg-in-hole problem on the example of force-torque maps," in *Proc. IEEE/RSJ Int. Conf. Intell. Robots Syst.*, 2010, pp. 2313–2318.

[14] Y. L. Yao and W. Y. Cheng, "Model-based motion planning for robotic assembly of non-cylindrical parts," *Int. J. Adv. Manuf. Technol.*, vol. 15, pp. 683–691, 1999.

[15] Y. Luo, X. Wang, M. Wang, D. Tan, T. Zhang, and Y. Yang, "A force/stiffness compensation method for precision multi-peg-hole assembly," *Int. J. Adv. Manuf. Technol.*, vol. 67, pp. 1–6, 2012.

[16] O. D. Faugerasand and M. Hebert, "The representation, recognition, and locating of 3-D Objects," *Int. J. Robot. Res.*, vol. 5, pp. 27–52, 1996.

[17] Z. Najdovski, S. Nahavandi, and T. Fukuda, "Design, development, and evaluation of a pinch-grasp haptic interface," *IEEE/ASME Trans. Mechatron.*, vol. 19, no. 1, pp. 45–54, Feb. 2014.

[18] L. Xin, M. Horie, and T. Kagawa, "Pressure-distribution methods for estimating lifting force of a swirl gripper," *IEEE/ASME Trans. Mechatron.*, vol. 19, no. 2, pp. 707–718, Apr. 2014.

[19] S. B. Backus and A. M. Dollar, "Robust resonant frequency-based contact detection with applications in robotic reaching and grasping," *IEEE/ASME Trans. Mechatron.*, vol. 19, no. 5, pp. 1552–1561, Oct. 2014.

[20] O. Skotheim, M. Lind, P. Ystgaard, and S. A. Fjerdingen, "A flexible 3D object localization system for industrial part handling," in *Proc. IEEE/RSJ Int. Conf. Intell. Robots Syst.*, 2012, pp. 3326–3333.

[21] D. Buchholz, M. Futterlieb, S. Winkelbach, and F. M. Wahl, "Efficient bin-picking and grasp planning based on depth data," in *Proc. IEEE Int. Conf. Robot. Autom.*, 2013, pp. 3245–3250.

[22] M. Y. Liu, O. Tuzel, A. Veeraraghavan, Y. Taguchi, T. K. Marks, and R. Chellappa, "Fast object localization and pose estimation in heavy clutter for robotic bin picking," *Int. J. Robot. Res.*, vol. 31, pp. 951–973, 2012.
[23] Y. M. Baek, S. Tanaka, and K. Harada, "Robust visual tracking of robotic forceps under a microscope using kinematic data fusion," *IEEE/ASME Trans. Mechatron.*, vol. 19, no. 1, pp. 278–288, Feb. 2014.
[24] V. Lippiello, F. Ruggiero, B. Siciliano, and L. Villani, "Visual grasp planning for unknown objects using a multifingered robotic Hand," *IEEE/ASME Trans. Mechatron.*, vol. 18, no. 3, pp. 1050–1059, Jun. 2013.
[25] J. F. Canny and K. Y. Goldberg, "RISC for industrial robotics: Recent results and open problems," in *Proc. IEEE Int. Conf. Robot. Autom.*, 1994, pp. 1951–1958.
[26] M. A. Erdmann, "Understanding action and sensing by designing action based sensors," *Int. J. Robot. Res.*, vol. 14, no. 5, pp. 483–509, 1995.
[27] R. H. Taylor, "A Synthesis of manipulator control programs from task-level specifications," Ph.D. dissertation, Artificial Intelligence Laboratory, Stanford University, Stanford, CA, USA, 1976.
[28] M. E. Caine, T. Lozano-Perez, and W. P. Seering, "Assembly strategies for chamferless parts," in *Proc. IEEE Int. Conf. Robot. Autom.*, 1989, vol. 1, pp. 472–477.
[29] T. Matsuno, T. Fukuda, and Y. Hasegawa, "Insertion of long peg into tandem shallow hole using search trajectory generation without force feedback," in *Proc. IEEE Int. Conf. Robot. Autom.*, 2004, vol. 2, pp. 1123–1128.
[30] M. T. Mason, "Compliant motion," *Robot Motion*. Cambridge, MA, USA: MIT Press, 1982.
[31] R. Zhang and K. Gupta, "Automatic orienting of polyhedra through step devices," in *Proc. IEEE Int. Conf. Robot. Autom.*, 1998, vol. 1, pp. 550–556.
[32] A. Marigo, M. Ceccarelli, S. Piccinocchi, and A. Bicchi, "Planning motions of polyhedral parts by rolling," *Algorithmica*, vol. 26, pp. 560–576, 2000.
[33] M. A. Erdmann and M. T. Mason, "An exploration of sensor-less manipulation," *IEEE J. Robot. Autom.*, vol. 4, no. 4, pp 369–370, Aug. 1988.
[34] K. F. Bohringer, V. Bhatt, B. R. Donald, and K. Goldberg, "Algorithms for sensorless manipulation using a vibrating surface," *Algorithmica*, vol. 26, pp. 389–429, 2000.
[35] R. P. Berretty, K. Goldberg, M. Overmars, and F. Van der Stappen, "Trap design for vibratory bowl feeders," *Int. J. Robot. Res.*, vol. 20, no. 11, pp. 891–908, 2001.
[36] M. T. Zhang and K. Y. Goldberg, "Gripper point contacts for part alignment," *IEEE Trans. Robot. Autom.*, vol. 18, no. 6, pp. 902–910, Dec. 2002.
[37] W. Kuperberg, "Problems on polytopes and convex sets," in *Proc. DIMACS Workshop Polytopes*, 1990, pp. 584–589.
[38] C. Davidson and A. Blake, "Caging planar objects with a three-finger one-parameter gripper," in *Proc. IEEE Int. Conf. Robot. Autom.*, 1998, vol. 3, pp. 2722–2727.
[39] P. Pipattanasomporn and A. Sudsang, "Two-finger caging of nonconvex polytopes," *IEEE Trans. Robot.*, vol. 27, no. 2, pp. 324–333, Apr. 2011.
[40] A. Rodriguez, M. T. Mason, and S. Ferry, "From caging to grasping," *Int. J. Robot. Res.*, vol. 31, pp. 886–900, 2012.
[41] J. Ponce, S. Sullivan, A. Sudsang, J. D. Boissonnat, and J. P. Merlet, "On computing four-finger equilibrium and force-closure grasps of polyhedral objects," *Int. J. Robot. Res.*, vol. 16, pp. 11–35, 1997.
[42] M. A. Roa and R. Suarez, "Computation of independent contact regions for grasping 3-D objects," *IEEE Trans. Robot.*, vol. 25, no. 4, pp. 839–850, Aug. 2009.
[43] H. Qiao, P. Moore, and J. Knight, "A model and strategy analysis of the peg-hole system in the search process associated with robotic assembly operations without chamfers," *Robotica*, vol. 14, pp. 647–658, 1996.
[44] H. Qiao, B. S. Dalay, and J. A. G. Knight, "Robotic assembly operation strategy investigation without force sensors through the research on contact point location and range of peg movement," *Proc. Inst. Mech. Eng. B, J. Eng. Manuf.*, vol. 210, pp. 471–485, 1996.
[45] H. Qiao and S. K. Tso, "Strategy investigation of precise robotic assembly operations with symmetric regular polyhedral objects," *Proc. Inst. Mech. Eng. B, J. Eng. Manuf.*, vol. 212, pp. 571–589, 1998.
[46] J. H. Su, H. Qiao, Z. C. Ou, and Y. R. Zhang, "Sensor-less insertion strategy for an eccentric peg in a hole of the crankshaft and bearing assembly," *Assembly Autom.*, vol. 32, pp. 86–99, 2012.
[47] S. Huang, Y. Yamakawa, T. Senoo, and M. Ishikawa, "Realizing peg-and-hole alignment with one eye-in-hand high-speed camera," in *Proc. IEEE/ASME Int. Conf. Adv. Intell. Mechatron.*, 2013, pp. 1127–1132.
[48] R. Usubamatov and K. Leong, "Analyses of peg-hole jamming in automatic assembly machines," *Assembly Autom.*, vol. 31, pp. 358–362, 2011.
[49] M. K. Vukobratovic and Y. Ekalo, "New approach to control of robotic manipulators interacting with dynamic environment," *Robotica*, vol. 14, no. 1, pp. 31–39, 1996.

Hong Qiao (SM'06) received the B.Eng. degree in hydraulics and control, the M.Eng. degree in robotics from Xian Jiaotong University, Xi'an, China, the M.Phil. degree in robotics control from the Industrial Control Center, University of Strathclyde, Strathclyde, U.K., and the Ph.D. degree in robotics and artificial intelligence from De Montfort University, Leicester, U.K., in 1995.

She was a University Research Fellow with De-Montfort University from 1995 to 1997. She was a Research Assistant Professor from 1997 to 2000 and an Assistant Professor from 2000 to 2002 with the Department of Manufacturing Engineering and Engineering Management, City University of Hong Kong, Kowloon, Hong Kong. In 2002, she joined as a Lecturer with the School of Informatics, University of Manchester, Manchester, U.K. She is currently a Professor with the State Key Laboratory of Management and Control for Complex Systems, Institute of Automation, Chinese Academy of Sciences, Beijing, China. She first proposed the concept of the attractive region in strategy investigation that she successfully applied for robot assembly, robot grasping, and part recognition, which is reported in *Advanced Manufacturing Alert* (New York, NY, USA: Wiley, 1999). Her current research interests include information-based strategy investigation, robotics and intelligent agents, animation, machine learning, and pattern recognition.

Dr. Qiao is currently a Member of the Administrative Committee of the IEEE Robotics and Automation Society (RAS), a Member of the IEEE Medal for Environmental and Safety Technologies Committee, and a Member of the Early Career Award Nomination Committee, Most Active Technical Committee Award Nomination Committee, and Industrial Activities Board for RAS. She is an Associate Editor of the IEEE TRANSACTIONS ON CYBERNETICS, and the IEEE TRANSACTIONS ON AUTOMATION SCIENCE AND ENGINEERING.

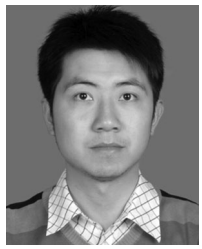

Min Wang received the B.Eng. degree from the University of Science and Technology of China, Hefei, China, in 2007, and the Ph.D. degree from the Institute of Automation, Chinese Academy of Sciences, Beijing, China, in 2012.

He is currently an Assistant Professor with the State Key Laboratory of Management and Control for Complex Systems, Institute of Automation, Chinese Academy of Sciences. His research interests include computer vision and intelligent robot system.

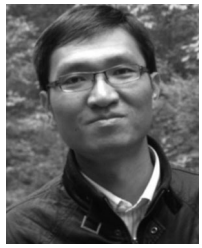

Jianhua Su received the B.Eng. degree in electronic and information engineering from Beijing Jiaotong University, Beijing, China, in 1999, the M.Eng. degree in electronic and information engineering from Beijing Jiaotong University, Beijing, in 2004, and the Ph.D. degree from the Institute of Automation, Chinese Academy of Sciences, Beijing, in 2009.

He is currently an Associate Professor with the Institute of Automation, Chinese Academy of Sciences. His background is in the fields of control theory, robotics, automation, and manufacturing. His current research interests include intelligent robot system and train control system.

Shengxin Jia received the B.Sc. and B.Eng. degrees in mechanical engineering from the Harbin Institute of Technology, Harbin, China, and from the University of Bath, Bath, U.K., respectively, in 2013. She is currently working toward the M.S. degree in mechanical engineering at the University of California, Los Angeles, CA, USA.

Her current research interests include application of attractive region in environment, machine design, and robot locomotion and manipulation.

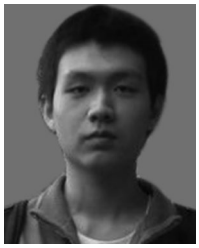

Rui Li received the B.Eng. degree in automation engineering from the University of Electronic Science and Technology of China, Chengdu, China, in 2013. He is currently working toward the Graduate degree with the Institute of Automation, Chinese Academy of Science, Beijing, China.

His current research interests include intelligent robot system and high-precision assembly.